AIP Journal of Applied Physics

Theory of substrate, Zeeman, and electron-phonon interaction effects on the quantum capacitance in graphene

M. Tahir, K. Sabeeh, A. Shaukat, and U. Schwingenschlögl

Citation: Journal of Applied Physics **114**, 223711 (2013); doi: 10.1063/1.4842755
View online: http://dx.doi.org/10.1063/1.4842755
View Table of Contents: http://scitation.aip.org/content/aip/journal/jap/114/22?ver=pdfcov
Published by the AIP Publishing

Theory of substrate, Zeeman, and electron-phonon interaction effects on the quantum capacitance in graphene

M. Tahir,[1,2] K. Sabeeh,[3] A. Shaukat,[2] and U. Schwingenschlögl[1,a)]
[1]*PSE Division, KAUST, Thuwal 23955-6900, Kingdom of Saudi Arabia*
[2]*Department of Physics, University of Sargodha, Sargodha 40100, Pakistan*
[3]*Department of Physics, Quaid-i-Azam University, Islamabad 45320, Pakistan*

(Received 30 September 2013; accepted 21 November 2013; published online 10 December 2013)

Since the discovery of graphene, a lot of interest has been attracted by the zeroth Landau level, which has no analog in the conventional two dimensional electron gas. Recently, lifting of the spin and valley degeneracies has been confirmed experimentally by capacitance measurements, while in transport experiments, this is difficult due to the scattering in the device. In this context, we model interaction effects on the quantum capacitance of graphene in the presence of a perpendicular magnetic field, finding good agreement with experiments. We demonstrate that the valley degeneracy is lifted by the substrate and by Kekule distortion, whereas the spin degeneracy is lifted by Zeeman interaction. The two cases can be distinguished by capacitance measurements. © *2013 AIP Publishing LLC*. [http://dx.doi.org/10.1063/1.4842755]

I. INTRODUCTION

Graphene, a single atomic sheet of graphite, has attracted much attention in condensed matter physics since the ground breaking experimental realization of this two dimensional system with unique properties.[1,2] It is a gapless semiconductor with conical electron and hole bands touching at the Fermi energy (E_F), such that the charge carriers thus obey a linear dispersion relation. This fundamental difference in the nature of the quasiparticles from conventional two dimensional electron gases (2DEGs) gives rise to phenomena such as the anomalous quantum Hall effect, Klein tunneling, and Berry physics.[3–11] Besides fundamental interest in understanding the electronic properties of graphene, there are substantiated suggestions that the material can serve as basis of nanoelectronic devices.[12–14] However, band gap engineering without destroying the essential structural properties is a significant challenge for applications.

In order to overcome this limitation, various ideas have been put forward including growth of graphene on specific substrates, such as hexagonal boron nitride (h-BN).[15–20] Being smooth on the atomic scale and endowed with a lattice constant close to graphene, h-BN has great advantages over other substrates, like SiO_2. Also, it is typically free of dangling bonds and charge traps. It has been demonstrated that graphene on h-BN shows an enhanced mobility together with reduced carrier inhomogeneities and roughness. A band gap has been observed in atomically thin films composed of h-BN and graphene.[17] Besides the band gap, the valley degeneracy of graphene is lifted.[21,22] Lifting of the spin and valley degeneracies, in general, has been addressed for electron-electron interaction,[23–27] electron-phonon interaction,[28–30] disorder,[31–33] and edge effects.[34,35] On the other hand, degeneracy lifting is difficult to probe by transport experiments due to scattering details.[20,36–39] In the following, we will address this issue by considering the quantum capacitance. In fact, recent quantum capacitance measurements have confirmed both the gap opening and lifting of the spin and valley degeneracies due to many body interactions in terms of the density of states (DOS).[40]

In the light the above, one of the most important tools for studying the electronic properties of solid state systems are capacitance measurements, as they can effectively probe the thermodynamic DOS of an electron system. The approach has been widely used for investigating conventional 2DEGs, see Refs. 41–43 and the references therein. Though graphene research has mainly focused on transport properties, for fundamental insight into the electronic structure as well as for device physics, it is also important to study the capacitance-voltage characteristics. This has been realized previously in the context of conventional 2DEGs and more recently in carbon nanotubes, graphene nanoribbons, and mono/bi-layer graphene.[44–49] Nowadays more attention is being paid to electrostatic properties such as the quantum capacitance of graphene devices.[40,50] Furthermore, from a device perspective, the potential of graphene as channel material to improve the performance of field effect transistors is creating excitement. This is due to the excellent intrinsic transport features and the possibility to pattern device structures by top-down lithographical techniques. Such devices consist of graphene on top of oxidized silicon or h-BN with source and drain electrodes attached, where the current through the device is controlled by a back gate. The capacitance in this case depends not only on the thickness of the insulating oxide layer (capacitive contribution C_{ins}) but also on the DOS of the graphene (quantum capacitance C_Q). The total capacitance C is obtained as $\frac{1}{C} = \frac{1}{C_{ins}} + \frac{1}{C_Q}$, where usually C_{ins} is the dominant contribution. However, in future devices with thinner oxide layers and higher dielectric constants, the quantum capacitance is expected to dominante.

The present work extends earlier capacitance studies of carbon based systems in the presence of a magnetic field.[50]

a)Udo.Schwingenschlogl@kaust.edu.sa. Tel.: +966-0544700080.

Starting from recent experimental work,[40] we model the combined effects of inversion symmetry breaking by a h-BN substrate, electron-phonon interaction, and a Zeeman field on the quantum capacitance of a graphene device. For an external magnetic field, by varying the gate voltage, we consider the lifting of the spin and valley degeneracies at the zeroth Landau level and the magnetic oscillations of the capacitance associated with the quantized Landau levels. The quantum capacitance is advantageous over traditional transport measurements[20,36–39] because it allows us to directly probe the DOS at the zeroth Landau level and is less sensitive to scattering details. We provide a quantitative description of the DOS at E_F and insight into the spin and valley splittings. Despite its capability to directly probe the electronic structure at finite temperature and magnetic field, the quantum capacitance so far has not been analyzed theoretically for graphene in the presence of interactions. Hence, a comprehensive study of interaction effects is undertaken in this work.

The paper is organized as follows: In Sec. II, we address substrate effects taking into account Gaussian broadening of the DOS to include the temperature. Section III deals with the combined effects in the presence of both a substrate and a Zeeman field. Moreover, we address in Sec. IV the combination of electron-phonon interaction and a Zeeman field and conclude in Sec. V.

II. SUBSTRATE

We consider a graphene sheet on a substrate in the xy-plane and an external magnetic field (B) applied along the z-direction. The corresponding two dimensional Dirac-like Hamiltonian[18–22] for an electron in the Landau gauge is $H = v(\eta\sigma_x \mathbf{p}_x + \sigma_y \mathbf{p}_y) + \Delta\sigma_z$. Here, $\sigma = (\sigma_x, \sigma_y, \sigma_z)$ is the vector of Pauli matrices, $\eta = +1/-1$ denotes the K/K′ valley, Δ is an energy term representing the substrate induced inversion symmetry breaking, v is the velocity of the Dirac states, and $\mathbf{p} = (\mathbf{p}_x, \mathbf{p}_y)$ is the two-dimensional canonical momentum. Using the Landau gauge with vector potential $(0, Bx, 0)$, the Landau levels are given by $E_n^\eta = t\sqrt{n\hbar^2\omega^2 + \Delta^2}$ for $n \neq 0$ and $E_0^\eta = -\eta\Delta$, where $\omega = v\sqrt{2eB/\hbar}$ is the cyclotron frequency, $t = +1/-1$ denotes electrons/holes, and n is an integer. The Landau level spectrum of Dirac electrons is significantly different from the spectrum of a conventional 2DEG, which is $E_n = \hbar\omega(n + 1/2)$, leading to different signatures of the quantum capacitance.

Capacitance oscillations in a magnetic field are directly related to the DOS at E_F. Without taking into account the disorder effects that are always present in real systems, the DOS can be expressed as a series of delta functions. To model scattering, we apply a Gaussian broadening of width Γ (zero shift) to the DOS

$$D(E) = \frac{2}{2\pi l^2}\frac{1}{\Gamma\sqrt{2\pi}}\sum_{\eta=\pm}\left(\exp\left[-\frac{(E-E_0^\eta)^2}{2\Gamma^2}\right] + \sum_{n=1}^{\infty}\exp\left[-\frac{(E-E_n^\eta)^2}{2\Gamma^2}\right]\right). \quad (1)$$

The DOS at E_F is obtained as

$$D(E=0) = \frac{1}{\pi l^2}\frac{1}{\Gamma\sqrt{2\pi}}\exp\left[-\frac{\Delta^2}{2\Gamma^2}\right] \times\left(1 + 2\sum_{n=1}^{\infty}\exp\left[-\frac{n\hbar^2\omega^2}{2\Gamma^2}\right]\right), \quad (2)$$

which can be further simplified using the relation $1 + 2\sum_{n=1}^{\infty}\exp[-2n\gamma] = \frac{1}{\tanh\gamma}$ with $\gamma = v^2\hbar eB/2\Gamma^2$

$$D(E=0) = \frac{\sqrt{2}\Gamma}{\pi^{3/2}v^2\hbar^2}\exp\left[-\frac{\Delta^2}{2\Gamma^2}\right]\frac{\gamma}{\tanh\gamma}. \quad (3)$$

For zero magnetic field, we have $\gamma/\tanh\gamma = 1$. We have an energy gap at E_F due to the inversion symmetry breaking induced by the substrate. Equation (3) agrees with Ref. 50 in the limit $\Delta = 0$.

To highlight the effects at E_F and the oscillations of the quantum capacitance for different magnetic fields and temperatures, we use the Poisson summation formula[51,52]

$$\frac{1}{2}F(0) + \sum_{k=1}^{\infty}F(k) = \int_0^{\infty}F(n)dn + 2\sum_{k=1}^{\infty}(-1)^k\int_0^{\infty}F(n)\cos[2\pi kn]dn. \quad (4)$$

The summation over n in Eq. (1) can be carried out by changing the variable to $x = \frac{E-\sqrt{n\hbar^2\omega^2+\Delta^2}}{\sqrt{2}\Gamma}$ and applying the limit $E \sim E_F = v\hbar k_F \gg \Gamma$, where $k_F = \sqrt{\pi n_e}$ denotes the Fermi wave vector and n_e is the carrier concentration in the system. The first integral yields $D_0 = \frac{|E|}{2\pi\hbar^2v^2}$, which is the DOS without magnetic field, and the second integral is

$$\int_{-\infty}^{\infty}dx\exp[-x^2]\cos\left[\frac{4\pi kE\Gamma}{\hbar^2\omega^2}x\right] = \sqrt{\pi}\exp\left[-\left(\frac{2\pi kE\Gamma}{\hbar^2\omega^2}\right)^2\right]. \quad (5)$$

We thus obtain for the Gaussian broadened DOS for $n \geq 1$

$$D(E) = D_0\left\{1 + 2\sum_{k=1}^{\infty}(-1)^k\exp\left[-\left(\frac{2\pi kE\Gamma}{\hbar^2\omega^2}\right)^2\right] \times\cos\left[2\pi k\frac{E^2-\Delta^2}{\hbar^2\omega^2}\right]\right\}. \quad (6)$$

Since the $k = 1$ term is sufficient to reproduce the experimental results in Fig. 3(a) of Ref. 50, we will focus in the following only on this term. The $n = 0$ level has to be treated separately according to Eq. (1).

For the temperature dependence of the quantum capacitance, we consider a device in which the capacitor is formed by the top gate and the graphene sheet. The quantum capacitance then represents the charge response in the channel as the gate voltage is varied, being defined as $C_Q \equiv \frac{e^2\partial Q}{\partial E_F} = \frac{e\partial n_e}{\partial E_F}$, where Q is the total charge on the graphene sheet. The gate

voltage is given by $V_g = \frac{E_F}{e}$. In conventional devices, C_Q is small and therefore can be ignored, whereas in nanoscale devices, it is the dominant capacitive contribution and consequently essential for designing purposes. The temperature dependent quantum capacitance for finite magnetic field can be written as[50,53]

$$C_Q = e^2 \int_0^\infty dE D(E) \frac{\partial f(E - E_F)}{\partial E_F}, \tag{7}$$

where $f(E - E_F)$ is the Fermi-Dirac distribution function. Changing the variable to $y = \beta(E - E_F)$ with $\beta = \frac{1}{k_B T}$ and applying the low temperature limit $\frac{1}{\beta} \ll E_F$, we find

$$C_Q = e^2 D_0 \left\{ 1 - \exp\left[-\left(\frac{2\pi E_F \Gamma}{\hbar^2 \omega^2} \right)^2 \right] \cos\left[\frac{2\pi E_F^2}{\hbar^2 \omega^2} \right] \times \int_0^\infty dy \frac{\cos\left[\frac{4\pi E_F}{\hbar^2 \omega^2 \beta} y \right]}{\cosh^2[y/2]} \right\}. \tag{8}$$

Evaluating the integral by the identity $\int_0^\infty dx \frac{\cos ax}{\cosh^2 bx} = \frac{a\pi}{2b^2 \sinh(a\pi/2b)}$ yields

$$C_Q = e^2 D_0 \left\{ 1 - 2 \frac{\alpha}{\sinh \alpha} \exp\left[-\left(\frac{2\pi E_F \Gamma}{\hbar^2 \omega^2} \right)^2 \right] \cos\left[\frac{2\pi E_F^2}{\hbar^2 \omega^2} \right] \right\}, \tag{9}$$

where $\alpha = \frac{4\pi^2 E_F}{\hbar^2 \omega^2 \beta}$ is a dimensionless parameter that expresses the characteristic temperature for the damping of oscillations in C_Q. The same approach yields for the temperature dependent quantum capacitance of a conventional 2DEG[41–43,51,52]

$$C_Q^{2DEG} = e^2 D_c \left\{ 1 - 2 \frac{\alpha_c}{\sinh \alpha_c} \exp\left[-2 \left(\frac{\pi \Gamma}{\hbar \omega} \right)^2 \right] \cos\left[\frac{2\pi E_F}{\hbar \omega} - \pi \right] \right\}, \tag{10}$$

where $D_c = \frac{m^*}{2\pi\hbar^2}$ and $\alpha_c = \frac{2\pi^2}{\hbar\omega\beta}$.

In order to compare the effects of temperature and the Gaussian broadening due to disorder on the quantum capacitance in graphene and conventional 2DEG devices, we analyze the differences between Eqs. (9) and (10): (1) The argument of the oscillatory term, $\cos\left[\frac{2\pi E_F}{\hbar\omega} - \pi \right]$, for the 2DEG depends on the ratio of the Fermi and cyclotron energies, whereas for graphene, it depends on the square of this ratio without phase shift. This can be attributed to the fact that the Dirac electrons in graphene acquiring a π Berry phase as they traverse a closed path in a magnetic field. (2) The exponential term responsible for the decay of the oscillation amplitude in the 2DEG case depends on the ratio of Γ and the cyclotron energy, whereas for graphene, it depends on the ratio of the product $E_F\Gamma$ and the cyclotron energy. The argument of the exponential term is 1.84 in the GaAs 2DEG but 0.22 in graphene for a magnetic field of 1 T and a disorder parameter of $\Gamma = 0.5$ meV. Therefore, in an experimentally relevant parameter range, disorder will cause less damping of the capacitance oscillations in a graphene device as compared to a conventional 2DEG device. (3) Since the effect of temperature on the oscillation is given by the factor $\lim_{\alpha\to\infty} \frac{\alpha}{\sinh(\alpha)} = 2\alpha e^{-\alpha}$, the amplitude decays exponentially as the temperature grows. For the characteristic temperature of the damping, we obtain $k_B T = \frac{veB}{2\pi^2 k_F}$, whereas in a conventional 2DEG,[41–43,51,52] the corresponding expression is $k_B T = \frac{\hbar\omega}{2\pi^2} = \frac{\hbar eB}{2\pi^2 m^*}$. For example, $m^* = 0.068 m_e$ in GaAs, where m_e is the electron mass. The ratio of the characteristic damping temperatures in graphene and conventional 2DEG devices is given by the ratio of the corresponding Fermi velocities. Typically, the Fermi velocity $\frac{\hbar k_F}{m^*}$ of a conventional 2DEG is 10^5 m/s and thus an order of magnitude smaller than that of graphene (10^6 m/s). Specifically, the ratio of the characteristic damping temperatures is $\frac{\hbar\sqrt{2\pi n_e}}{vm^*} = 0.24$ for GaAs, 0.03 for Ge, and 0.015 for Si, with $n_e = 3.2 \times 10^{15}$ m^{-2}. To obtain the same temperature scale, the effective mass of the carriers in the conventional 2DEG is required to be 0.016 m_e, which is very small.

From the above discussion, we expect that the capacitance oscillations are less affected by the temperature in the graphene than in the conventional 2DEG case, due to the higher characteristic damping temperature. In the following, we employ numerical results for GaAs for comparison. When the magnetic field varies, the Landau levels cross E_F one by one, leading to Shubnikov de Haas oscillations in the quantum capacitance. By the proportionality to the DOS, an exponential decay of the oscillation amplitude with temperature and disorder is expected. The quantum capacitance is plotted as function of the dimensionless magnetic field B_0/B in Fig. 1, using $B_0 = \hbar k_F^2 = 13.25$ T for $n_e = 3.2 \times 10^{15}$ m^{-2} and the realistic parameters $\Gamma = \sqrt{B}\,\text{meV}/\sqrt{\text{T}}$ and $T = 1.2$ K.[41–43,50–52] The Shubnikov de Haas oscillations in the graphene case are found to be enhanced and less damped with temperature as compared to the conventional 2DEG case. There is a π Berry phase difference, whereas the period and frequency are the same in the two systems. For the parameters considered here, the oscillations are found to be almost completely damped around 20 K for the conventional 2DEG, whereas they persist beyond 100 K for graphene.

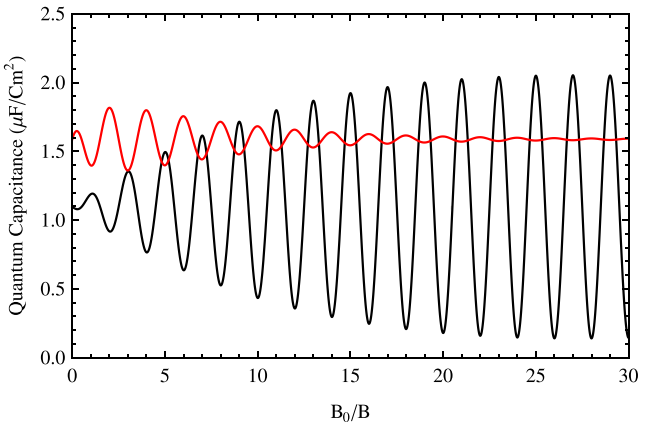

FIG. 1. Quantum capacitance as a function of the inverse magnetic field for a temperature of 1.2 K. The black line represents the graphene monolayer and the red line the conventional 2DEG.

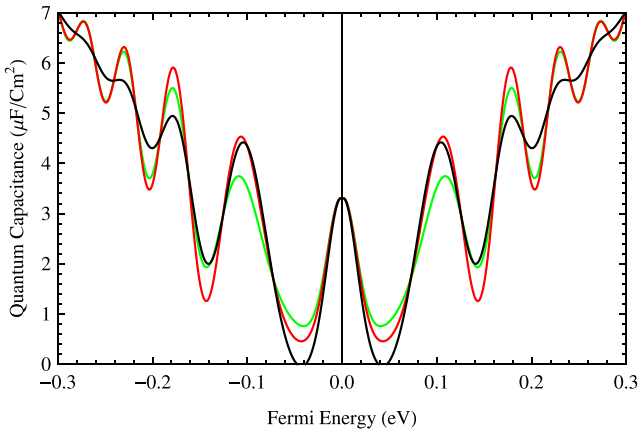

FIG. 2. Quantum capacitance as a function of the Fermi energy for $\Delta = 0$ meV. The temperature is 15 K (green line), 35 K (red line), and 100 K (black line), and the magnetic field is 16 T.

For field effect transistors using graphene as channel material, it is also important to determine the effect of V_g. To this end, we plot in Fig. 2 the quantum capacitance as a function of $E_F = eV_g$. We set $B = 16$ T and address temperatures of 15, 35, and 100 K. A realistic impurity concentration of $n_i = 2 \times 10^{11}\,\mathrm{cm}^{-2}$ (Ref. 50) yields $\Gamma = 15$ meV, since $\Gamma \sim \frac{\hbar}{\tau}$ with $\tau = \frac{30\sqrt{\pi n_e}}{\pi^2 v n_i}$ and $n_e = 3.2 \times 10^{12}\,\mathrm{cm}^{-2}$ in graphene.[54–56] Variation of V_g shifts E_F and populates/depopulates successively the Landau levels, leading to Shubnikov de Haas oscillations. The quantum capacitance shows a maximum at the Dirac point with oscillations superimposed on a linear increase to both sides. The electron-hole symmetry[50] is clearly visible. In order to see the effects of the symmetry breaking induced by the substrate, we demonstrate in Fig. 3 that a gap develops at the Dirac point when we increase Δ, while keeping all other parameters as in Fig. 2. This gap even exists in the absence of a magnetic field, consistent with the experimental observation in Ref. 20. Our Landau level broadening of $\Gamma = 15$ meV enables a direct comparison with the experimental results in Fig. 3 of Ref. 50. The charge inhomogeneity reported in this reference is due to the sample size and SiO_2 substrate but does not apply to a h-BN substrate.[40]

III. SUBSTRATE AND ZEEMAN FIELD

Adding a Zeeman exchange field breaks the spin symmetry of the system, in each valley independently. The Hamiltonian is modified to $H = v(\eta\sigma_x \mathbf{p}_x + \sigma_y \mathbf{p}_y) + \Delta\sigma_z + M\sigma_z$, where $M = g\mu_B \mathrm{B}$ is the Zeeman energy with $g = 2$ and the Bohr magneton μ_B. We obtain the eigenvalues $E_n^{s,\eta} = t\sqrt{n\hbar^2\omega^2 + \Delta^2} + sM$ for $n \neq 0$ and $E_0^{s,\eta} = -\eta\Delta + sM$ with $s = +1/-1$ representing spin up/down. The quantum capacitance for the $n = 0$ Landau level then is

$$C_Q(n=0) = \frac{e^2}{2\pi l^2}\frac{1}{\Gamma\sqrt{2\pi}}\sum_{s,\eta}\exp\left[-\frac{(E+\eta\Delta - sM)^2}{2\Gamma^2}\right]. \tag{11}$$

For higher Landau levels, we employ the same procedure as before and obtain

$$C_Q = e^2 D_0\left\{1/2 - \sum_s \frac{\alpha_s}{\sinh\alpha_s}\exp\left[-\left(\frac{2\pi(E_F - sM)\sqrt{2}\Gamma}{\hbar^2\omega^2}\right)^2\right] \times\cos\left[2\pi\frac{(E_F - sM)^2 - \Delta^2}{\hbar^2\omega^2}\right]\right\}, \tag{12}$$

with $\alpha_s = \frac{4\pi^2(E_F - sM)}{\hbar^2\omega^2\beta}$.

By Eq. (11), the four-fold degeneracy of the zeroth Landau level is lifted when the valley degeneracy is lifted by the substrate and the spin degeneracy by the Zeeman field. Accordingly, Fig. 4 shows as a function of E_F for the zeroth Landau level four peaks with an energy gap in the middle, using the parameters $\Delta = 10$ meV, $T = 15$ K, and $\Gamma = 1$ meV.[38,40] For increasing magnetic field (10 T, 20 T, 40 T), the Zeeman spin splitting evolves consistent with experiments.[36] Spin and valley splittings can be verified by the quantum capacitance. While the effects of a Zeeman field[36] and of a h-BN substrate[20] have been observed separately in transport experiments so far, investigation of the combined effect is possible by quantum capacitance experiments.[40] Discriminating the lifting of the spin and valley degeneracies is possible by means of a substrate combined with

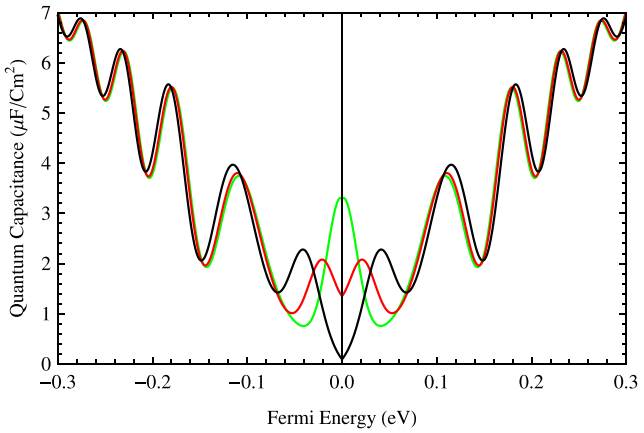

FIG. 3. Quantum capacitance as a function of the Fermi energy for different values of Δ: 0 meV (green line), 20 meV (red line), and 40 meV (black line). The temperature is 15 K and the magnetic field is 16 T.

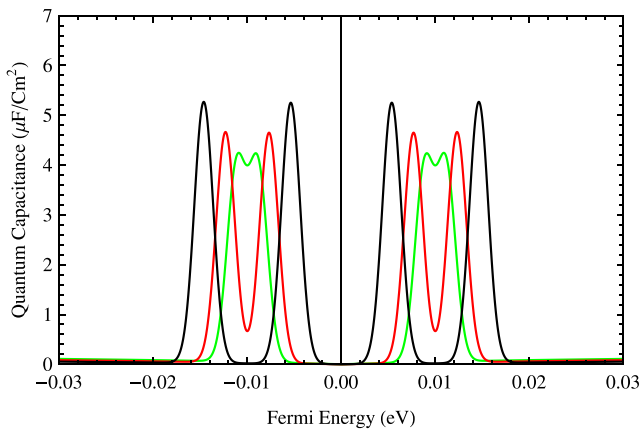

FIG. 4. Quantum capacitance as a function of the Fermi energy for $\Delta = 10$ meV. The magnetic field is 10 T (green line), 20 T (red line), and 40 T (black line), and the temperature is 15 K.

a Zeeman field. An energy gap at E_F is important for device operations and for controlling the transport in graphene based nanoelectronics.

IV. KEKULE DISTORTION AND ZEEMAN FIELD

It recently has been proposed that a spontaneous Kekule deformation of the graphene structure can occur as a consequence of the coupling between the in-plane optical phonons and the electronic degrees of freedom,[30,57] leading to an energy gap of $2\Delta_0$, see below. This essentially breaks the inversion symmetry and the valley degeneracy is lifted, similar to the effects of a substrate but smaller in magnitude. We consider graphene (suspended sample) in the presence of a Zeeman field to study the electron-phonon interaction. While electron-phonon effects frequently have been subject of experimental and theoretical investigations, we are interested in the consequences for the quantum capacitance. The eigenvalues of the meanfield Kekule Hamiltonian are[30] $E_n^s = t\sqrt{n\hbar^2\omega^2 + \Delta_0^2} + sM$ for $n \neq 0$ and $E_0^{s,\eta} = \eta\Delta_0 + sM$, where Δ_0 is the electron-phonon coupling energy due to Kekule distortion. The quantum capacitance for the $n=0$ Landau level then is

$$C_Q(n=0) = \frac{e^2}{2\pi l^2}\frac{1}{\Gamma\sqrt{2\pi}}\sum_{s,\eta}\exp\left[-\frac{(E-\eta\Delta_0 - sM)^2}{2\Gamma^2}\right], \tag{13}$$

and for higher Landau levels, we obtain analogously to the previous procedure the same result as in Eq. (12).

The combination of Kekule deformation and Zeeman energy does not only lift the spin and valley degeneracies for this level but also influences the transport properties. We employ a realistic value of $2M$ for the electron-phonon energy[30,57] and of 1 meV for the disorder broadening.[36] Disorder broadening has been discussed in detail in Refs. 4 and 58 and the DOS in Refs. 56 and 59. Motivated by experimental difficulties to understand the zeroth Landau level in terms of the quantum capacitance, we show that this level is robust against temperature and disorder, in agreement with room temperature experiments.[60] In the limit of zero Zeeman field, it splits into two levels separated by an energy gap, as observed in scanning tunneling spectroscopy.[29] Being proportional to the DOS, the experimental spectrum is directly related to our results. We note that it is straightforward to extend the experiment to a Zeeman field and the corresponding quantum phase transitions, as done before by quantum capacitance measurements.[40] The numerical results are analogous to Fig. 4 just with the Kekule parameter (Δ_0) replacing the substrate term (Δ). It is possible to distinguish between the liftings of the spin and valley degeneracies.

V. CONCLUSION

We have investigated the quantum capacitance of a device with graphene as channel material, taking into account temperature and disorder induced Gaussian broadening of the Landau levels. The results obtained are compared to a conventional 2DEG. The Shubnikov de Haas oscillations under variation of the magnetic field are found to be enhanced and more robust against the temperature in the graphene case for which an additional π Berry phase shift is observed. A metal-insulator transition is induced by the broken inversion symmetry if the graphene is mounted on a substrate as well as for Kekule distortion. We have studied the combined effects of substrate and Zeeman field, showing a lifting of the spin and valley degeneracies of the zeroth Landau level. While discrimination between spin and valley degeneracy lifting is not possible in standard transport experiments, quantum capacitance measurements will enable discrimination if a combination of either a substrate or a Kekule distortion with a Zeeman field is employed. Therefore, such measurements are important for the design of nanoscale devices based on graphene and for gaining insight into the spin and valley polarizations.

[1]K. S. Novoselov, A. K. Geim, S. V. Morozov, D. Jiang, Y. Zhang, S. V. Dubonos *et al.*, "Electric field effect in atomically thin carbon films," Science **306**, 666–669 (2004).
[2]K. S. Novoselov, A. K. Geim, S. V. Morozov, D. Jiang, M. I. Katsnelson, I. V. Grigorieva *et al.*, "Two-dimensional gas of massless Dirac fermions in graphene," Nature **438**, 197–200 (2005).
[3]Y. Zhang, Y. W. Tan, H. L. Stormer, and P. Kim, "Experimental observation of the quantum Hall effect and Berry's phase in graphene," Nature **438**, 201–204 (2005).
[4]Y. Zheng and T. Ando, "Hall conductivity of a two-dimensional graphite system," Phys. Rev. B **65**, 245420 (2002).
[5]V. P. Gusynin and S. G. Sharapov, "Unconventional integer quantum Hall effect in graphene," Phys. Rev. Lett. **95**, 146801 (2005).
[6]N. M. R. Perez, F. Guinea, and A. H. Castro Neto, "Electronic properties of disordered two-dimensional carbon," Phys. Rev. B **73**, 125411 (2006).
[7]M. I. Katsnelson, K. S. Novoselov, and A. K. Geim, "Chiral tunnelling and the Klein paradox in graphene," Nat. Phys. **2**, 620–625 (2006).
[8]K. S. Novoselov, E. McCann, S. V. Morozov, V. I. Fal'ko, M. I. Katsnelson, U. Zeitler *et al.*, "Unconventional quantum Hall effect and Berry's phase of 2π in bilayer graphene," Nat. Phys. **2**, 177–180 (2006).
[9]T. Ohta, A. Bostwick, T. Seyller, K. Horn, and E. Rotenberg, "Controlling the electronic structure of bilayer graphene," Science **313**, 951–954 (2006).
[10]J. B. Oostinga, H. B. Heersche, X. Liu, A. F. Morpurgo, and L. M. K. Vandersypen, "Gate-induced insulating state in bilayer graphene devices," Nature Mater. **7**, 151–157 (2008).
[11]A. H. C. Neto, F. Guinea, N. M. R. Peres, K. S. Novoselov, and A. K. Geim, "The electronic properties of graphene," Rev. Mod. Phys. **81**, 109–162 (2009).
[12]C. Berger, Z. Song, X. Li, X. Wu, N. Brown, C. Naud *et al.*, "Electronic confinement and coherence in patterned epitaxial graphene," Science **312**, 1191–1196 (2006).
[13]R. S. Deacon, K. C. Chuang, R. J. Nicholas, K. S. Novoselov, and A. K. Geim, "Cyclotron resonance study of the electron and hole velocity in graphene monolayers," Phys. Rev. B **76**, 081406(R) (2007).
[14]S. Y. Zhou, G. H. Gweon, J. Graf, A. V. Fedorov, C. D. Spataru, R. D. Diehl *et al.*, "First direct observation of Dirac fermions in graphite," Nat. Phys. **2**, 595–599 (2006).
[15]G. Giovannetti, P. A. Khomyakov, G. Brocks, P. J. Kelly, and J. v. Brink, "Substrate-induced band gap in graphene on hexagonal boron nitride: Ab initio density functional calculations," Phys. Rev. B **76**, 073103 (2007).
[16]C. R. Dean, A. F. Young, I. Meric, C. Lee, L. Wang, S. Sorgenfrei *et al.*, "Boron nitride substrates for high-quality graphene electronics," Nat. Nanotechnol. **5**, 722–726 (2010).
[17]L. Ci, L. Song, C. Jin, D. Jariwala, D. Wu, Y. Li *et al.*, "Atomic layers of hybridized boron nitride and graphene domains," Nature Mater. **9**, 430–435 (2010).
[18]P. M. Krstajić and P. Vasilopoulos, "Integer quantum Hall effect in gapped single-layer graphene," Phys. Rev. B **86**, 115432 (2012).
[19]J. Jung, Z. Qiao, Q. Niu, and A. H. MacDonald, "Transport properties of graphene nanoroads in boron nitride sheets," Nano Lett. **12**, 2936–2940 (2012).

[20]F. Amet, J. R. Williams, K. Watanabe, T. Taniguchi, and D. G. Gordon, "Insulating behavior at the neutrality point in single-layer graphene," Phys. Rev. Lett. **110**, 216601 (2013).
[21]D. Xiao, W. Yao, and Q. Niu, "Valley-contrasting physics in graphene: Magnetic moment and topological transport," Phys. Rev. Lett. **99**, 236809 (2007).
[22]A. Rycerz, J. Tworzydlo, and C. W. J. Beenakker, "Valley filter and valley valve in graphene," Nat. Phys. **3**, 172–175 (2007).
[23]V. P. Gusynin, V. A. Miransky, and I. A. Shovkovy, "Catalysis of dynamical flavor symmetry breaking by a magnetic field in 2 + 1 dimensions," Phys. Rev. Lett. **73**, 3499 (1994).
[24]H. A. Fertig and L. Brey, "Luttinger liquid at the edge of undoped graphene in a strong magnetic field," Phys. Rev. Lett. **97**, 116805 (2006).
[25]V. P. Gusynin, V. A. Miransky, S. G. Sharapov, and I. A. Shovkovy, "Excitonic gap, phase transition, and quantum Hall effect in graphene," Phys. Rev. B **74**, 195429 (2006).
[26]D. V. Khveshchenko, "Magnetic-field-induced insulating behavior in highly oriented pyrolitic graphite," Phys. Rev. Lett. **87**, 206401 (2001).
[27]J. Alicea and M. P. A. Fisher, "Graphene integer quantum Hall effect in the ferromagnetic and paramagnetic regimes," Phys. Rev. B **74**, 075422 (2006).
[28]J. N. Fuchs and P. Lederer, "Spontaneous parity breaking of graphene in the quantum hall regime," Phys. Rev. Lett. **98**, 016803 (2007).
[29]G. Li, A. Luican, and E. Y. Andrei, "Scanning tunneling spectroscopy of graphene on graphite," Phys. Rev. Lett. **102**, 176804 (2009).
[30]C. Y. Hou, C. Chamon, and C. Mudry, "Deconfined fractional electric charges in graphene at high magnetic fields," Phys. Rev. B **81**, 075427 (2010).
[31]K. Nomura and A. H. MacDonald, "Quantum Hall ferromagnetism in graphene," Phys. Rev. Lett. **96**, 256602 (2006).
[32]M. O. Goerbig, R. Moessner, and B. Doucot, "Electron interactions in graphene in a strong magnetic field," Phys. Rev. B **74**, 161407 (2006).
[33]D. A. Abanin, P. A. Lee, and L. S. Levitov, "Randomness-induced XY ordering in a graphene quantum Hall ferromagnet," Phys. Rev. Lett. **98**, 156801 (2007).
[34]A. H. Castro Neto, F. Guinea, and N. M. R. Peres, "Edge and surface states in the quantum Hall effect in graphene," Phys. Rev. B **73**, 205408 (2006).
[35]D. A. Abanin, P. A. Lee, and L. S. Levitov, "Spin-filtered edge states and quantum Hall effect in graphene," Phys. Rev. Lett. **96**, 176803 (2006).
[36]Y. Zhang, Z. Jiang, J. P. Small, M. S. Purewal, Y. W. Tan, M. Fazlollahi *et al.*, "Landau-level splitting in graphene in high magnetic fields," Phys Rev. Lett. **96**, 136806 (2006).
[37]J. G. Checkelsky, L. Li, and N. P. Ong, "Divergent resistance at the Dirac point in graphene: Evidence for a transition in a high magnetic field," Phys. Rev. B **79**, 115434 (2009).
[38]Y. Zhao, P. C. Zimansky, F. Ghahari, and P. Kim, "Magnetoresistance measurements of graphene at the charge neutrality point," Phys. Rev. Lett. **108**, 106804 (2012).
[39]A. F. Young, C. R. Dean, L. Wang, H. Ren, P. C. Zimansky, K. Watanabe *et al.*, "Spin and valley quantum Hall ferromagnetism in graphene," Nat. Phys. **8**, 550–556 (2012).
[40]G. L. Yu, R. Jalil, B. Belle, A. S. Mayorov, P. Blake, F. Schedin *et al.*, "Interaction phenomena in graphene seen through quantum capacitance," Proc. Natl. Acad. Sci. U.S.A. **110**, 3282–3286 (2013).
[41]T. Ando, A. B. Fowler, and F. Stern, "Electronic properties of two-dimensional systems," Rev. Mod. Phys. **54**, 437–672 (1982).
[42]A. Isihara, "Low temperature properties of two-dimensional electrons," Phys. Scr. **32**, 26 (1985).
[43]A. Isihara and L. Smrcka, "Density and magnetic field dependences of the conductivity of two-dimensional electron systems," J. Phys. C **19**, 6777 (1986).
[44]S. Ilani, L. A. K. Donev, M. Kindermann, and P. L. McEuen, "Measurement of the quantum capacitance of interacting electrons in carbon nanotubes," Nat. Phys. **2**, 687–691 (2006).
[45]J. Guo, Y. Yoon, and Y. Ouyang, "Gate electrostatics and quantum capacitance of graphene nanoribbons," Nano Lett. **7**, 1935–1940 (2007).
[46]T. Fang, A. Konar, H. L. Xing, and D. Jena, "Carrier statistics and quantum capacitance of graphene sheets and ribbons," Appl. Phys. Lett. **91**, 092109 (2007).
[47]A. A. Shylau, J. W. Kłos, and I. V. Zozoulenko, "Capacitance of graphene nanoribbons," Phys. Rev. B **80**, 205402 (2009).
[48]J. Xia, F. Chen, J. Li, and N. Tao, "Measurement of the quantum capacitance of graphene," Nat. Nanotechnol. **4**, 505–509 (2009).
[49]F. Giannazzo, S. Sonde, V. Raineri, and E. Rimini, "Screening length and quantum capacitance in graphene by scanning probe microscopy," Nano Lett. **9**, 23–29 (2009).
[50]L. A. Ponomarenko, R. Yang, R. V. Gorbachev, P. Blake, A. S. Mayorov, K. S. Novoselov *et al.*, "Density of states and zero Landau level probed through capacitance of graphene," Phys. Rev. Lett. **105**, 136801 (2010).
[51]R. B. Dingle, "Some magnetic properties of metals. II. The influence of collisions on the magnetic behaviour of large systems," Proc. R. Soc. London, Ser. A **211**, 517–525 (1952).
[52]A. Isihara and L. Smrcka, "Effects of level broadening on the magneto-thermal oscillations in two-dimensional electron systems," J. Phys. C **18**, 4703 (1985).
[53]M. Tahir and U. Schwingenschlögl, "Beating of magnetic oscillations in a graphene device probed by quantum capacitance," Appl. Phys. Lett. **101**, 013114 (2012).
[54]T. Stauber, N. M. Peres, and F. Guinea, "Electronic transport in graphene: A semiclassical approach including midgap states," Phys. Rev. B **76**, 205423 (2007).
[55]S. Cho and M. S. Fuhrer, "Charge transport and inhomogeneity near the minimum conductivity point in graphene," Phys. Rev. B **77**, 081402 (2008).
[56]W. Zhu, Q. W. Shi, X. R. Wang, J. Chen, J. L. Yang, and J. G. Hou, "Shape of disorder-broadened Landau subbands in graphene," Phys. Rev. Lett. **102**, 056803 (2009).
[57]K. Nomura, S. Ryu, and D. H. Lee, "Field-induced Kosterlitz-Thouless transition in the N = 0 Landau level of graphene," Phys. Rev. Lett. **103**, 216801 (2009).
[58]P. M. Krstajić and P. Vasilopoulos, "Integral quantum Hall effect in graphene: Zero and finite Hall field," Phys. Rev. B **83**, 075427 (2011).
[59]W. Zhu, H. Y. Yuan, Q. W. Shi, J. G. Hou, and X. R. Wang, "Shape of the Landau subbands in disordered graphene," Phys. Rev. B **83**, 153408 (2011).
[60]K. S. Novoselov, Z. Jiang, Y. Zhang, S. V. Morozov, H. L. Stormer, U. Zeitler *et al.*, "Room-temperature quantum Hall effect in graphene," Science **315**, 1379 (2007).